Reggies/flotillins regulate E-cadherin–mediated cell contact formation by affecting EGFR trafficking

Gonzalo P. Solis*,†, Yvonne Schrock*, Nikola Hülsbusch*, Marianne Wiechers, Helmut Plattner, and Claudia A. O. Stuermer
Department of Biology, University of Konstanz, 78467 Konstanz, Germany

ABSTRACT **The reggie/flotillin proteins are implicated in membrane trafficking and, together with the cellular prion protein (PrP), in the recruitment of E-cadherin to cell contact sites. Here, we demonstrate that reggies, as well as PrP down-regulation, in epithelial A431 cells cause overlapping processes and abnormal formation of adherens junctions (AJs). This defect in cell adhesion results from reggie effects on Src tyrosine kinases and epidermal growth factor receptor (EGFR): loss of reggies reduces Src activation and EGFR phosphorylation at residues targeted by Src and c-cbl and leads to increased surface exposure of EGFR by blocking its internalization. The prolonged EGFR signaling at the plasma membrane enhances cell motility and macropinocytosis, by which junction-associated E-cadherin is internalized and recycled back to AJs. Accordingly, blockage of EGFR signaling or macropinocytosis in reggie-deficient cells restores normal AJ formation. Thus, by promoting EGFR internalization, reggies restrict the EGFR signaling involved in E-cadherin macropinocytosis and recycling and regulate AJ formation and dynamics and thereby cell adhesion.**

Monitoring Editor
Asma Nusrat
Emory University

Received: Dec 12, 2011
Revised: Feb 16, 2012
Accepted: Mar 14, 2012

INTRODUCTION

Adhesion between epithelial cells typically depends on the adhesion molecule E-cadherin and its linkage to the actin cytoskeleton through the intracellular ligands α-, β-, and p120-catenin (Nishimura and Takeichi, 2009). Disturbances in E-cadherin function can cause epithelial tumor progression to invasiveness and metastasis (Gavard and Gutkind, 2008). A major factor underlying impaired cell adhesion and thus cancer is elevation of epidermal growth factor (EGF) and EGF receptor (EGFR) signaling through which many crucial signal transduction molecules are (over-) activated (Gavard and Gutkind, 2008). This imbalanced signaling affects many cellular functions, including increase in cell motility and decrease in cell adhesion, by modifying regulators of the E-cadherin/catenin complex or its internalization and turnover (Mosesson *et al.*, 2008). In intact tissues, the adhesion-disrupting influence of EGFR signaling is restricted by efficient EGFR internalization and down-regulation (Sorkin and Goh, 2008).

The spatiotemporally controlled internalization and turnover of the E-cadherin/catenin complex is necessary for the maintenance of cell adhesion, which prevents extensive cell overlap (Green *et al.*, 2010). Thus, although seemingly stable, the adhesive contacts between cells are continually remodeled. Within cell contact sites, E-cadherin is typically concentrated in adherens junctions (AJs), which are highly dynamic structures and subject to a continuous basal-to-apical flow (Kametani and Takeichi, 2007). Concurrently, E-cadherin molecules in AJs are continually turned over (Hong *et al.*, 2010). Bryant *et al.* (2007) demonstrated that E-cadherin at cell contact sites is internalized by macropinocytosis, recycled, and redelivered to the plasma membrane (PM) without degradation. It is not known, however, whether this process affects cell adhesion, and its regulation is still not well understood, but macropinocytosis apparently internalizes the E-cadherin/catenin complex as a whole. Macropinocytosis is an effective way to incorporate in a clathrin-independent manner segments of membrane that are redelivered to distinct sites of the cell (Falcone *et al.*, 2006). Typical activators of

This article was published online ahead of print in MBoC in Press (http://www.molbiolcell.org/cgi/doi/10.1091/mbc.E11-12-1006) on March 21, 2012.

*These authors contributed equally to this work.

†Present address: Department of Pharmacology and Toxicology, University of Lausanne, CH-1005 Lausanne, Switzerland.

The authors declare no conflict of interest.

Address correspondence to: Gonzalo P. Solis (Gonzalo.Solis@unil.ch), Claudia A.O. Stuermer (Claudia.Stuermer@uni-konstanz.de).

Abbreviations used: AJ, adherens junction; EGFR, epidermal growth factor receptor; PM, plasma membrane; PrP, prion protein; shRNA, short hairpin RNA; siRNA, small interfering RNA; WT, wild type.

macropinocytosis in epithelial cells are EGF, as well as phosphatidylinositol 3-kinase (PI3K) and Rac1, downstream of EGFR signaling (Falcone *et al.*, 2006).

E-cadherin plays a major role during tissue reorganization and migration in the developing embryo (Halbleib and Nelson, 2006). Only recently has it been recognized in zebrafish embryos that the recruitment of E-cadherin from intracellular Rab11-positive vesicles to cell contact sites depends on prion protein (PrP)–PrP *trans*-interaction and the ensuing signal transduction (Malaga-Trillo *et al.*, 2009). Because PrP associates with reggie microdomains (Solis *et al.*, 2010), these data raised the question of whether reggies would affect E-cadherin functions in mammalian epithelial cells.

The reggie proteins (also known as flotillins) are expressed in virtually every cell type and across organisms as distant as fly and human (Stuermer, 2010). Although this suggests that they subserve basic cellular functions, precisely which roles reggies play has remained elusive. That reggies are crucial for membrane trafficking and turnover came from evidence in neurons, where they are necessary for growth cone elongation (Munderloh *et al.*, 2009). Furthermore, participation of reggies in signal transduction has been repeatedly reported (Stuermer, 2010). Reggies interact with Src tyrosine kinases and adaptor proteins of the ponsin family. Together they activate the ubiquitin ligase c-cbl and the GTPase TC10 and control the exocyst-assisted translocation of membrane proteins (Kioka *et al.*, 2002). Evidence from the literature, together with results from our own work, recently led to the hypothesis that reggies regulate the recruitment and targeted delivery of specific membrane proteins from intracellular compartments to specific sites of the PM (Stuermer, 2010). This attributes to reggies a role in cargo trafficking and accounts for the fact that reggies are essential for growth cone elongation, neuronal differentiation, and axon regeneration (Munderloh *et al.*, 2009). Of interest, reggies have been implicated in a clathrin- and dynamin-independent endocytic route of the glycosylphosphatidylinositol-anchored protein CD59 (Glebov *et al.*, 2006). Furthermore, reggies have also been shown to facilitate clathrin-dependent endocytosis of the amyloid precursor protein and the transporters of cholesterol and dopamine (Schneider *et al.*, 2008; Cremona *et al.*, 2011; Ge *et al.*, 2011).

In the present study we set out to clarify whether reggies might contribute to the internalization, turnover, trafficking, and targeted deployment of E-cadherin and whether they might regulate cell adhesion in association with PrP. Our results show that reggie down-regulation inhibits EGFR internalization by blocking the phosphorylation of two of its major tyrosine phosphorylation sites (Y1045 and Y845) and disturbs cell adhesion and AJ formation and dynamics. This defect in AJ formation and dynamics is caused by an imbalanced rate of the macropinocytic uptake and redelivery of E-cadherin to AJs. Accordingly, AJs can be rescued by amiloride, Rac1, and PI3K inhibition, all known inhibitors of macropinocytosis. Reggies are not required for macropinosome formation, but instead regulate, together with PrP, the targeted recycling of E-cadherin to AJs.

RESULTS

The role of reggies in E-cadherin–mediated cell contact formation

Human A431 epidermoid carcinoma cells naturally express E-cadherin and coaccumulate reggie-1, PrP, and E-cadherin at cell contacts (Figure 1, A and B). As shown for other cell types (Langhorst *et al.*, 2008), reggie-1 also occurs at several types of vesicles. To determine the role of reggie-1 and PrP in cell contact formation, we generated permanently transfected A431 cell lines by using short hairpin RNA (shRNA) vectors against reggie-1 and PrP (hereafter

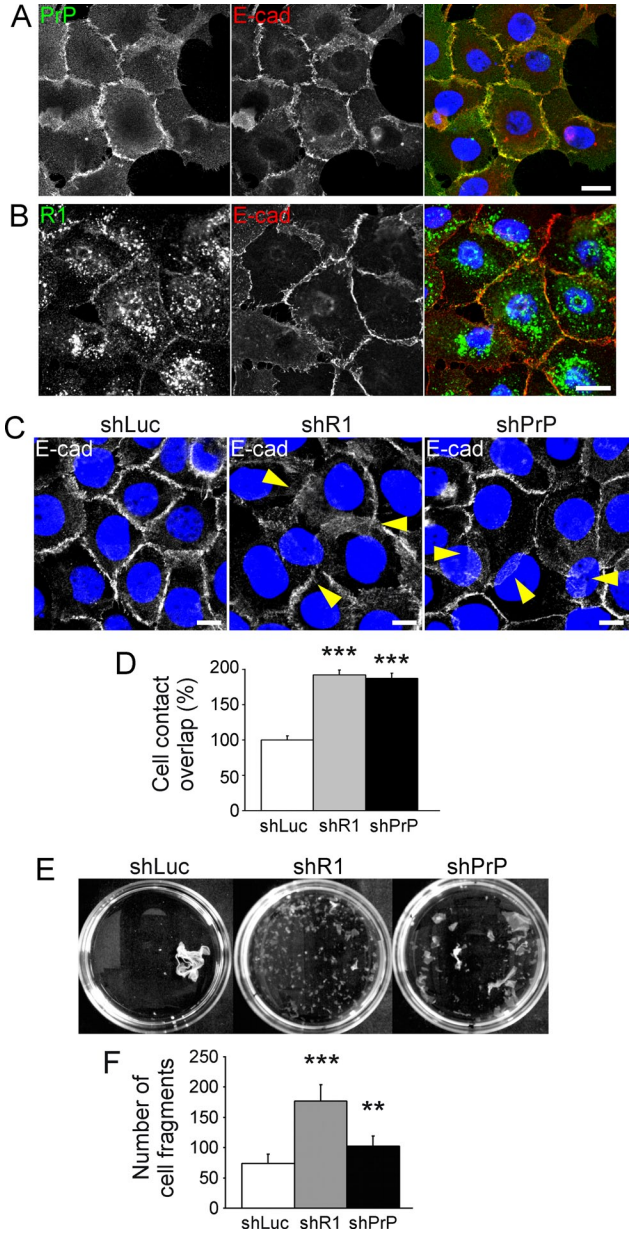

FIGURE 1: Reggies regulate cell contact inhibition and intercellular adhesion in A431 cells. Immunostaining of endogenous PrP (A) and reggie-1 (R1, B) showed that both proteins colocalized with E-cadherin (E-cad) at cell contact sites in A431 cells. Scale bars, 10 µm. (C) Down-regulation of reggie-1 (shR1) or PrP (shPrP) induced a significant increase in overlapping processes (yellow arrowheads) as revealed by E-cad immunostaining. Scale bars, 10 µm. (D) Quantification of overlapping areas (n = 3, ***p < 0.001, one-way ANOVA, mean ± SEM). (E) Intercellular adhesion was analyzed using the dispase-based dissociation assay. Whereas a low degree of fragmentation of the cell carpets was observed in control shLuc cells (left), increased levels of fragmentation were apparent in shR1 (middle) and shPrP (right) cells. (F) Quantification of the dispase assay (n = 4, **p < 0.01, ***p < 0.001, one-way ANOVA, mean ± SEM).

shR1 and shPrP, respectively). Of interest, down-regulation of reggie-1 not only affected the expression of reggie-2 (Solis *et al.*, 2007), but also decreased the protein levels of PrP (Supplemental Figure S1, A and B). Conversely, PrP ablation seemed not to affect the levels of both reggie-1 and -2 (Supplemental Figure S1, A and B). shR1

and shPrP cells were organized in small clusters and retained cell contacts like wild-type (WT) and shRNA control cells (hereafter sh-Luc; Supplemental Figure S2A). E-cadherin immunostaining of shRNA-transfected cells did not show any apparent abnormality. However, both shR1 and shPrP cells formed overlapping processes with neighboring cells of an area twice as large as shLuc cells (Figure 1, C and D). No other defects, such as in cell size, shape, or number, were observed in shR1 and shPrP cells (unpublished data). This result suggests that reggies and PrP are involved in E-cadherin–mediated contact formation in A431 cells, consistent with findings in zebrafish embryos (Malaga-Trillo *et al.*, 2009). Similar phenotypes were observed in cell contacts of MCF-7 mammary epithelial cells and E-cadherin–enhanced green fluorescent protein (EGFP)–expressing HeLa cells treated with small interfering RNAs (siRNAs) against reggie-1 or PrP (Supplemental Figure S2, B and C).

To analyze whether the increase in overlapping processes observed in shR1 and shPrP cells affects intercellular adhesion, we used the dispase-based dissociation assay (Huen *et al.*, 2002). Although shLuc cell carpets exhibited only minimal dissociation, shR1, as well as shPrP, cell carpets dissociated into numerous smaller fragments after mechanical stress (Figure 1, E and F). Thus down-regulation of reggies or PrP leads to impaired cell adhesion.

Biochemical analyses of shR1 and shPrP cells revealed that the cell adhesion defects were not due to an impaired expression of E-cadherin, β-catenin, or p120-catenin nor of caveolin-1, as another lipid raft protein (Supplemental Figure S1A). Moreover, neither were reggie-1 and PrP required for the formation of the E-cadherin/catenin complex (Supplemental Figure S1C) nor was the cell surface E-cadherin expression significantly affected in shR1 and shPrP cells, as shown by biotinylation and trypsinization experiments (Supplemental Figure S1, D and E). Because a fraction of E-cadherin has been reported to associate with lipid rafts (Seveau *et al.*, 2004) and reggies are raft components, we analyzed the E-cadherin raft distribution in A431 cells. However, the amount of E-cadherin in lipid raft fractions was very small in these cells and was not visibly affected upon down-regulation of reggies or PrP (Supplemental Figure S1F). Of interest, we observed approximately twofold increase in the tyrosine phosphorylation level of β-catenin (Supplemental Figure S1G) but not that of p120-catenin or E-cadherin in shR1 and shPrP cells (unpublished data). To test whether down-regulation of reggies or PrP would affect the level of E-cadherin endocytosis, surface proteins were biotinylated and cells incubated for 2 h at 37°C. After stripping of the residual surface biotinylated proteins, the internalized E-cadherin was determined. Western blots showed that the pool of internalized E-cadherin in shR1 and shPrP cells was not different from that in control cells (Supplemental Figure S1H). Thus reggies and PrP appear not to control the overall E-cadherin surface localization, its binding with the major catenins, or its raft association.

The role of reggies in the formation, organization, and dynamics of AJs

Given that down-regulation of reggies did not cause an overall reduction of E-cadherin at the PM, we reasoned that perhaps specific elements, the AJs, might be affected. A431 cells treated with 0.2% Triton X-100 before fixation selectively retain E-cadherin stabilized in AJs, which appear as streaks (Shewan *et al.*, 2005). In WT and control shLuc cells, detergent-resistant E-cadherin staining appeared in prominent streaks at cell contacts, which colocalized with the ends of perijunctional actin bundles and partially with reggie-1 and PrP (Figure 2A and Supplemental Figure S3, A–C). However, in contrast to WT and shLuc cells, detergent-resistant AJs appeared strongly

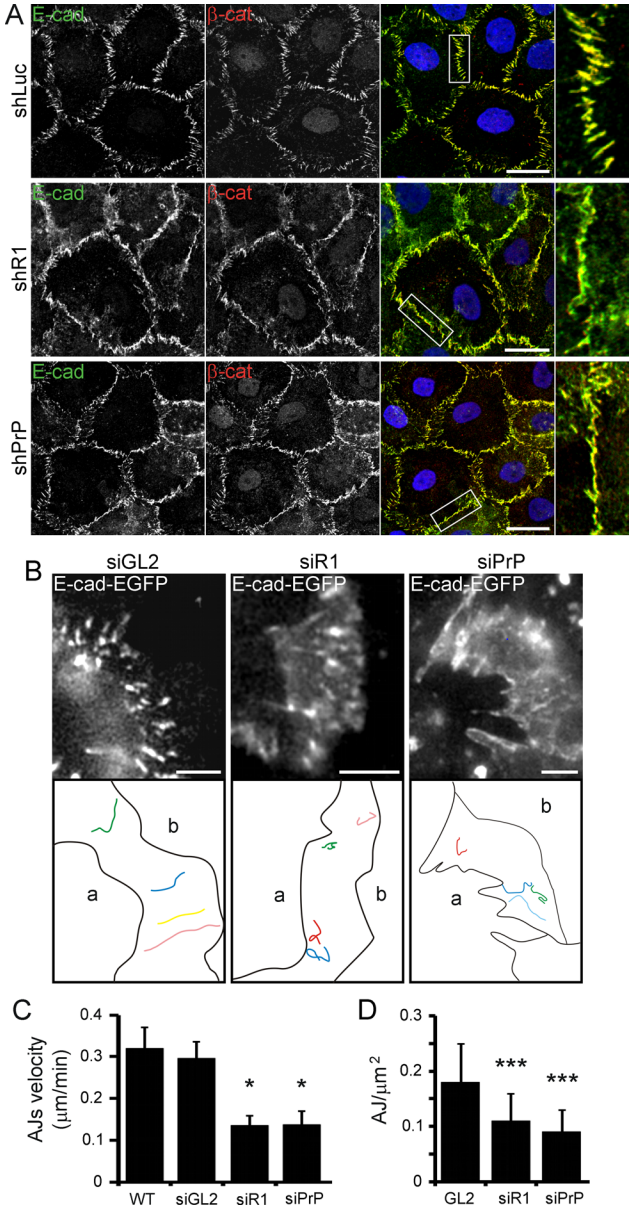

FIGURE 2: Disruption of AJ formation and dynamics after reggie-1 and PrP down-regulation. (A) Immunostainings of the detergent-resistant pools of E-cadherin (E-cad) and β-catenin (β-cat) showed the streaks typical of AJs at contact sites in control A431 cells (shLuc, first row) and revealed disorganized AJs in reggie-1 (shR1, second row) and PrP (shPrP, third row) knockdown cells (enlargement of boxed areas on the right). Scale bars, 10 μm. (B) E-cadherin–EGFP (E-cad-EGFP)–expressing cells were transfected with control siRNA (siGL2), siRNA against reggie-1 (siR1), or siRNA against PrP (siPrP) and AJ movements recorded for 20 min. In contrast to control cells (left), AJs were not well defined, and their basal-to-apical movements were significantly reduced in siR1 (middle) and siPrP (right) cells. Trajectories of individual AJs from basal (b) to apical (a) regions of overlapping cell contacts (outlined by black lines) are shown in color (bottom). Scale bars, 5 μm. (C, D) Quantifications showed a significant reduction of velocity (C) and number (D) of AJs in cells treated as in B ($n = 5$, $^*p < 0.05$, $^{***}p < 0.001$, one-way ANOVA, mean ± SEM).

disorganized in shR1 and shPrP cells: AJs were often not evident, and a diffuse E-cadherin distribution was observed along the entire contact sites (Figure 2A). By contrast, the formation and organization of desmosomes were not affected in shR1 and shPrP cells

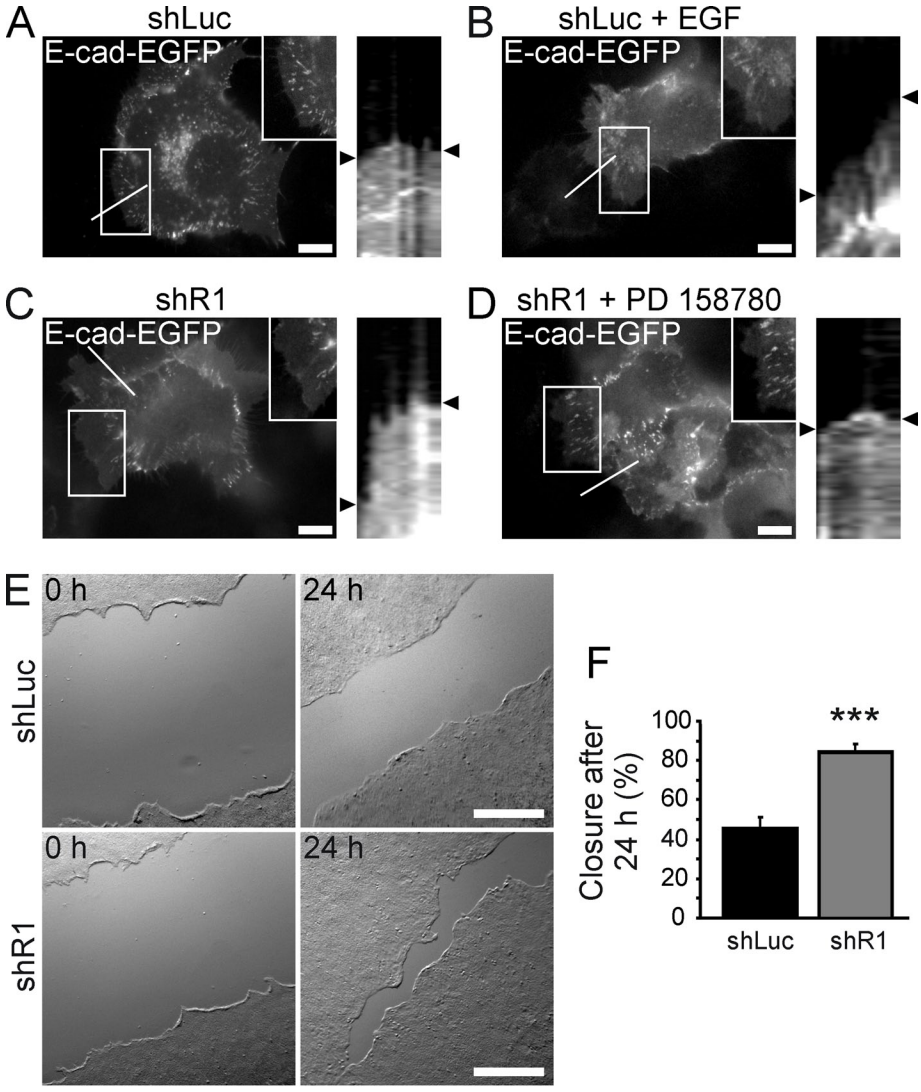

FIGURE 3: EGFR blocker rescued AJ formation defects of shR1 cells. (A–D) E-cadherin–EGFP (E-cad-EGFP) expression in shRNA stably transfected A431 cells revealed the reduction in AJ formation (boxed area enlarged in inserts) and increased cell motility (white lines and kymographs on the right) in shR1 cells (C) compared with control shLuc cells (A). Stimulation of shLuc cells with 10 ng/ml EGF (B) mimicked both the reduced AJ formation and the increased cell motility observed in shR1 cells. Incubation of shR1 cells with the EGFR blocker PD 158780 (D) rescued the defects in AJ formation and increased cell motility. Selected areas showed cell contacts between E-cad-EGFP–expressing and nontransfected cells for better visualization. Scale bars, 5 μm. (E) A scratch assay showed an increased invasion and wound closure after 24 h in shR1 over shLuc cells, which is quantified in F. Scale bar, 500 μm. (F) Quantification of scratch closure after 24 h (n = 4, ***$p < 0.001$, *t* test, mean ± SEM).

(Supplemental Figure S3D), suggesting that the defects in cell adhesion result from an impaired E-cadherin–dependent AJ formation.

To obtain independent evidence for defects in AJ morphology, we analyzed the apparent length of AJs at the electron microscopic (EM) level (Supplemental Figure S3E). AJs in shR1 cells (0.32 ± 0.03 μm, n = 31) were significantly shorter than their counterparts in shLuc cells (0.54 ± 0.06 μm; p = 0.008, n = 29). Likewise, AJs in shPrP cells were also reduced in length compared with control shLuc cells (0.37 ± 0.04 μm; p = 0.05, n = 19).

It has recently been shown in A431 cells that AJs are highly dynamic structures, which continuously form at the base of cell contact sites, migrate apically within a few minutes, and are then internalized (Hong *et al.*, 2010). To analyze the role of reggies in AJ dynamics, we generated a permanently transfected A431 cell line expressing E-cadherin–EGFP and transfected these cells with a specific siRNA against reggie-1. Time-lapse microscopy studies showed that, in fact, E-cadherin–labeled AJs moved from the basal to the apical aspect of cell contacts in a very well-organized manner in WT and control siRNA–transfected cells (Figure 2B and Supplemental Movie S1). As expected, AJs appeared strongly disorganized in cells transfected with siRNA against reggie-1: individual AJs were often not visible, and a rather homogeneous fluorescence was observed over the entire contact site (Figure 2B and Supplemental Movie S2). Accordingly, the amount of AJs visible at cell contacts was significantly reduced in these cells (Figure 2D). Of note, the AJs that did form were markedly impaired in their coordinated basal-to-apical movement (Figure 2B). Individual AJs normally move with an average velocity of 0.32 ± 0.05 μm/min in WT and 0.30 ± 0.04 μm/min in control transfected cells, which fell to 0.14 ± 0.02 μm/min in cells transfected with siRNA against reggie-1 (Figure 2C). A very similar phenotype was observed in cells treated with siRNA against PrP (Figure 2, B and D, and Supplemental Movie S3), confirming the functional association between reggie-1 and PrP.

Taken together, these data indicate that the expression of reggies (and PrP) is necessary for adhesive strength, the correct formation and organization of AJs, and the coordinated movement of AJs at contact sites.

The role of reggies in EGFR endocytosis and signaling

It is well known that cell adhesion is impaired as a consequence of increased EGFR activity (Gavard and Gutkind, 2008). Therefore we examined whether increased EGFR signaling might be responsible for the defects in AJs observed in shR1 cells.

Of interest, EGFR immunostaining revealed its colocalization with E-cadherin–EGFP in AJs at cell contact sites (especially at the most apical region), suggesting a functional relationship between EGF signaling and AJ formation (Supplemental Figure S4A). When control shLuc cells were exposed to 10 ng/ml EGF, AJ formation was impaired, mimicking the phenotype observed in shR1 cells (Figure 3, A–C, and Table 1). Whereas higher EGF concentrations showed stronger effects on AJ formation, lower concentrations only partially mimicked the shR1 phenotype (unpublished data). Of note, the defects in AJs observed in shR1 cells were fully rescued by incubation with the specific EGFR blockers tyrphostin AG-1478 and PD158780 (Figure 3, C and D, and Table 1), strongly indicating that reggies affect AJ formation by regulating EGFR signaling.

Because cell adhesion is often inversely correlated with cell motility, we examined whether ruffling activity and wound-closure

	Number of AJs (AJ/μm²)	Cell motility (μm/min)
shLuc	0.170 ± 0.014	0.060 ± 0.000
shLuc + EGF	0.073 ± 0.015***	0.108 ± 0.019*
shR1	0.043 ± 0.009***	0.138 ± 0.023*
shR1 + PD158780	0.162 ± 0.013	0.060 ± 0.000
shR1 + tyrphostin AG-1478	0.154 ± 0.010	n.d.

EGF stimulation of control shLuc cells mimicked the defect in AJ formation (number of AJs) and cell motility observed in shR1 cells. EGFR inhibitors (PD158780 and tyrphostin AG-1478) rescued both AJ and cell motility defects in shR1 cells. n.d., Data not determined. Statistical differences related to shLuc cells. n = 3, *p < 0.05, ***p < 0.001, one-way ANOVA, mean ± SEM.

TABLE 1: Quantification of AJs and cell motility.

dynamics were altered in shR1 cells. Cell motility was increased in shR1 cells, and this was mimicked by EGF stimulation of control shLuc cells (Figure 3, A–C, and Table 1). On the other hand, the increased cell motility observed in shR1 cells was rescued by the specific EGFR blocker (Figure 3D and Table 1). Moreover, when a scratch was applied to cell monolayers, the wound was closed two times faster in shR1 than in shLuc cells (Figure 3, E and F). Thus down-regulation of reggies additionally increased cell motility and migration.

To determine whether EGFR expression and signaling are perturbed when reggies are missing, we analyzed shLuc and shR1 cells upon EGF stimulation. Whereas most EGFR staining was lost from the PM in control cells after 120 min of EGF application, the receptor remained at the PM and in intracellular compartments in shR1 cells (Figure 4A and Supplemental Figure S4B). To verify the specificity of this effect, we performed a rescue experiment by transfecting shR1 cells with a reggie-1–EGFP shRNA–resistant construct. Whereas EGFR immunostaining accumulated at the PM in untransfected shR1 cells after EGF stimulation, the receptor was efficiently down-regulated in those cells into which reggie-1 was reintroduced (Figure 4B). Conversely, the expression of caveolin-1–EGFP did not rescue the defects in EGFR down-regulation in shR1 cells (Supplemental Figure S4C), indicating that the absence of reggies cannot be compensated for by this lipid raft component.

Likewise, in a biochemical experiment in which the cell surface proteins were biotinylated, EGFR was strongly increased in the pool of cell surface proteins after stimulation with EGF in shR1 and shPrP cells compared with control shLuc cells (Figure 4, C and D). However, only a moderate but significant increase in the total level of the receptor was observed in shR1 and shPrP cells upon stimulation (Figure 4, C and D). These results suggest that reggies and PrP regulate EGFR endocytosis after EGF stimulation, and, therefore, its reduced internalization in shR1 and shPrP cells caused a delay in receptor degradation. To confirm this hypothesis, we indirectly quantified EGFR endocytosis using rhodamine-labeled EGF. As expected, shR1 cells exhibited 30 and 40% reduced EGF uptake after 5 and 10 min of incubation, respectively (Figure 4, E and F). Thus reggies appear to control the internalization of EGFR during EGF stimulation. However, reggie-1 did not significantly colocalize either with EGFR or EGF-rhodamine–labeled vesicles after 5 min of stimulation (Figure 4G; Langhorst *et al.*, 2008), indicating that reggies regulate receptor internalization but are not at vesicles along the major EGFR endocytic pathway.

EGFR activity is tightly controlled and regulated by tyrosine phosphorylation at multiple sites of the receptor. Therefore we examined whether reggies might contribute to the tyrosine phosphorylation state of EGFR upon EGF stimulation. Western blots were performed with antibodies specific for the phosphorylated EGFR tyrosine residues 845, 992, 1045, 1068, and 1148, respectively. In addition to the expected delay in EGFR degradation (Figure 5, A and B), the absence of reggies caused a strong reduction in the phosphorylation of Y845 and Y1045 and had milder effects on other tyrosine residues (Figure 5, A and C). Y1045 is the major autophosphorylation residue of EGFR and is involved in c-cbl–dependent EGFR ubiquitination and internalization (Sorkin and Goh, 2008). Consistently, we observed that shR1 cells showed reduced c-cbl immunostaining at the PM after 5 min of EGF stimulation (Supplemental Figure S4D). EGFR phosphorylation at the Y845 residue was reported to depend on Src activity (Leu and Maa, 2003). Therefore we analyzed the level of activated Src using specific antibodies against the activated forms of the kinases. Indeed, shR1 cells showed an overall reduced level in activated Src kinases compared with control shLuc cells (Figure 6, A and B).

Next we studied whether the impaired EGFR internalization observed in shR1 cells may affect downstream signaling molecules known to require EGFR signaling in endosomes (Murphy *et al.*, 2009). Accordingly, during EGF stimulation the activation of Erk1/2, PI3K, and Akt was significantly reduced in shR1 cells, whereas p38 MAPK activation was enhanced (Figure 6, A and B). In addition, we observed that the levels of reggie-1 slightly decrease during EGF stimulation of control shLuc cells (Figures 5A and 6A); however, this effect was not significant.

Taken together, the present observations suggest that the impaired cell adhesion upon down-regulation of reggies seems to result from delayed EGFR endocytosis, which, in turn, might induce a sustained EGFR activity at the PM.

Reggies and macropinocytosis

Our results indicate that the defective AJ formation in shR1 cells is caused by elevated surface EGFR signaling without noticeable effects on the ratio of E-cadherin at the PM versus intracellular pools. Still, AJs are E-cadherin–dependent structures and are characterized by continuous E-cadherin turnover (Hong *et al.*, 2010). It has been reported that in EGF-stimulated MCF-7 cells the level of surface-exposed E-cadherin is kept at steady state through its internalization by macropinocytosis and recycling (Bryant *et al.*, 2007). Therefore we examined macropinosome formation and E-cadherin trafficking in shR1 and control shLuc cells and tested whether its macropinocytic uptake and deployment at AJs might be affected by reggies.

To determine whether reggies are involved in macropinocytosis, we applied EGF-rhodamine to reggie-1-EGFP–expressing A431 cells. By 5 min after stimulation, cells exhibited the typical ring-shaped macropinocytic structures containing both EGF and reggie-1 (Figure 7A). These macropinosomes also contained endogenous reggie-1, EGFR, and E-cadherin, together with β-catenin and p120, as well as PrP (Figure 7, B–D, and Supplemental Figure S5, A–D).

When we examined whether the absence of reggies affects macropinocytosis, we found that shR1 cells did exhibit macropinosomes after EGF application (Supplemental Figure S5, B–D). Thus reggies are apparently not necessary for macropinosome formation. By contrast, shR1 cells showed macropinosomes with an apparently higher frequency than shLuc cells (unpublished data), indicating that depletion of reggies promotes macropinosome formation. For a semiquantitative assessment, we stimulated shR1 and control shLuc cells with EGF in the presence of high–molecular

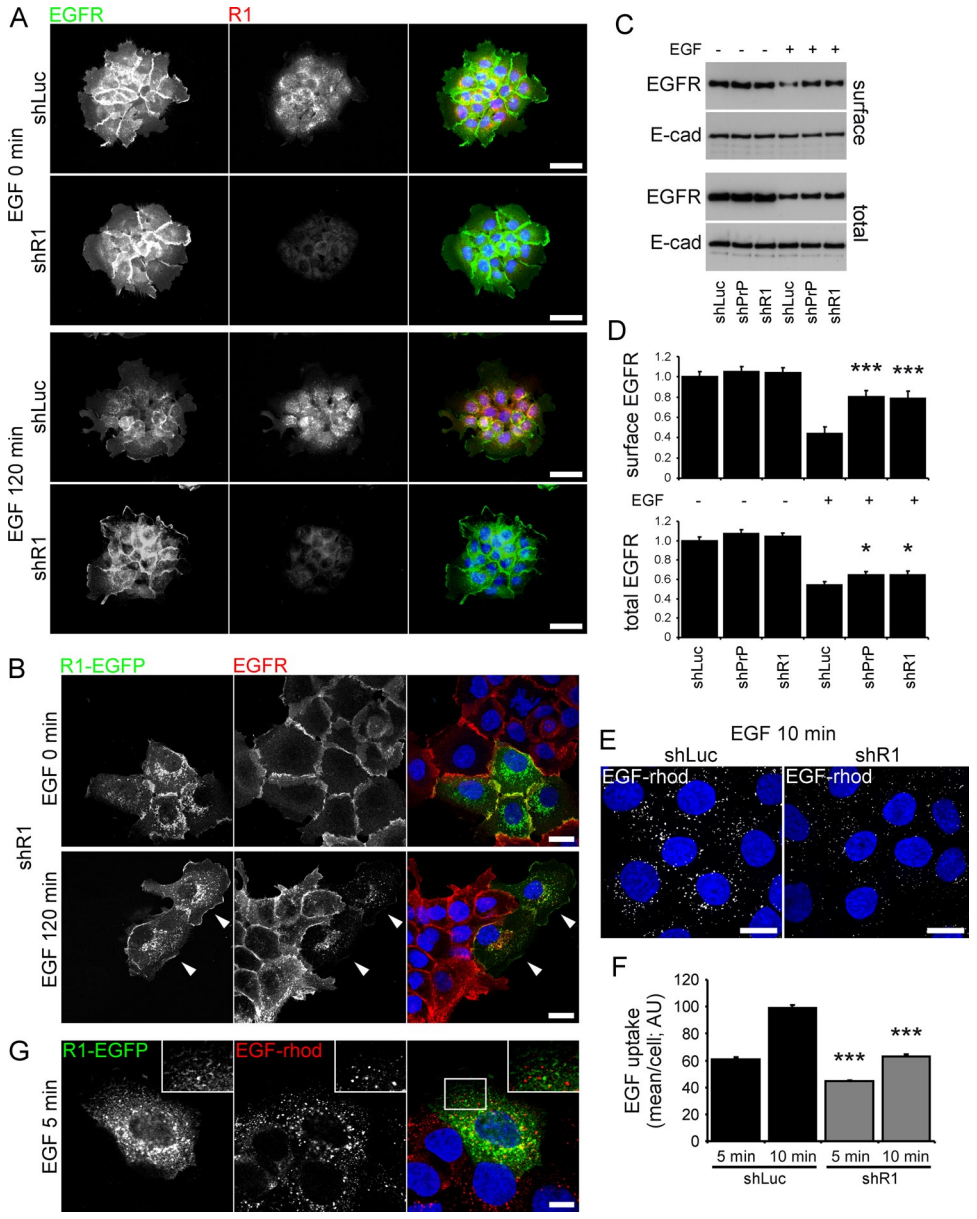

FIGURE 4: Reggies regulate EGFR internalization. (A) EGFR immunostaining is densest at cell contact sites in control shLuc and shR1 cells at resting state (0 min EGF). When stimulated with 10 ng/ml EGF for 120 min, EGFR staining is strongly reduced in shLuc cells but not in shR1 cells. Scale bars, 20 μm. (B) When reggie-1 is reintroduced (R1-EGFP) into shR1 cells in a rescue experiment, EGFR staining is reduced in R1-EGFP–expressing cells (white arrowheads) after stimulation with EGF (120 min). Scale bars, 10 μm. (C, D) 120 min of EGF application (+) leads to a strong reduction of EGFR from the cell surface in shLuc control cells but significantly less in shR1 and shPrP cells, whereas E-cadherin remains unchanged. When the total amount of EGFR is determined after EGF stimulation a significant reduction occurs in all cells due to receptor degradation but less in shR1 and shPrP cells compared with the shLuc controls (n = 3, *p < 0.05, ***p < 0.001, one-way ANOVA, mean ± SEM). (E) Exposure of cells to EGF-rhodamine (EGF-rhod) for 10 min led to significant endocytosis in shLuc control cells as evidenced by the large number of rhodamine-labeled endosomes. This uptake was partially blocked in shR1 cells. (F) Quantification of EGF-rhodamine uptake at 5 and 10 min of exposure to EGF as explained in E (n = 3, ***p < 0.001, paired *t* test, mean ± SEM). Scale bars, 10 μm. (G) EGF-rhodamine containing endosomes after 5 min of treatment were not colocalized with reggie-1 (R1-EGFP) at the cell periphery (boxed area enlarged in inserts) to any significant extent. Scale bars, 10 μm.

weight Alexa-labeled dextran, which is typically endocytosed by macropinosomes (Kerr and Teasdale, 2009). A comparison between cells showed that shR1 cells internalized dextran more efficiently than did shLuc cells (Figure 7, E and F), implying that the absence of reggies promotes macropinocytic uptake. Accordingly, the same effect was observed in shPrP cells (Supplemental Figure S6, A and B). This increased macropinocytosis in shR1 and shPrP cells can be explained by the persistence of EGFR at the PM upon EGF stimulation. The fact that reggie-1 associates with but is not necessary for macropinosome formation suggests that reggies may play a role in the trafficking of macropinocytic cargo proteins.

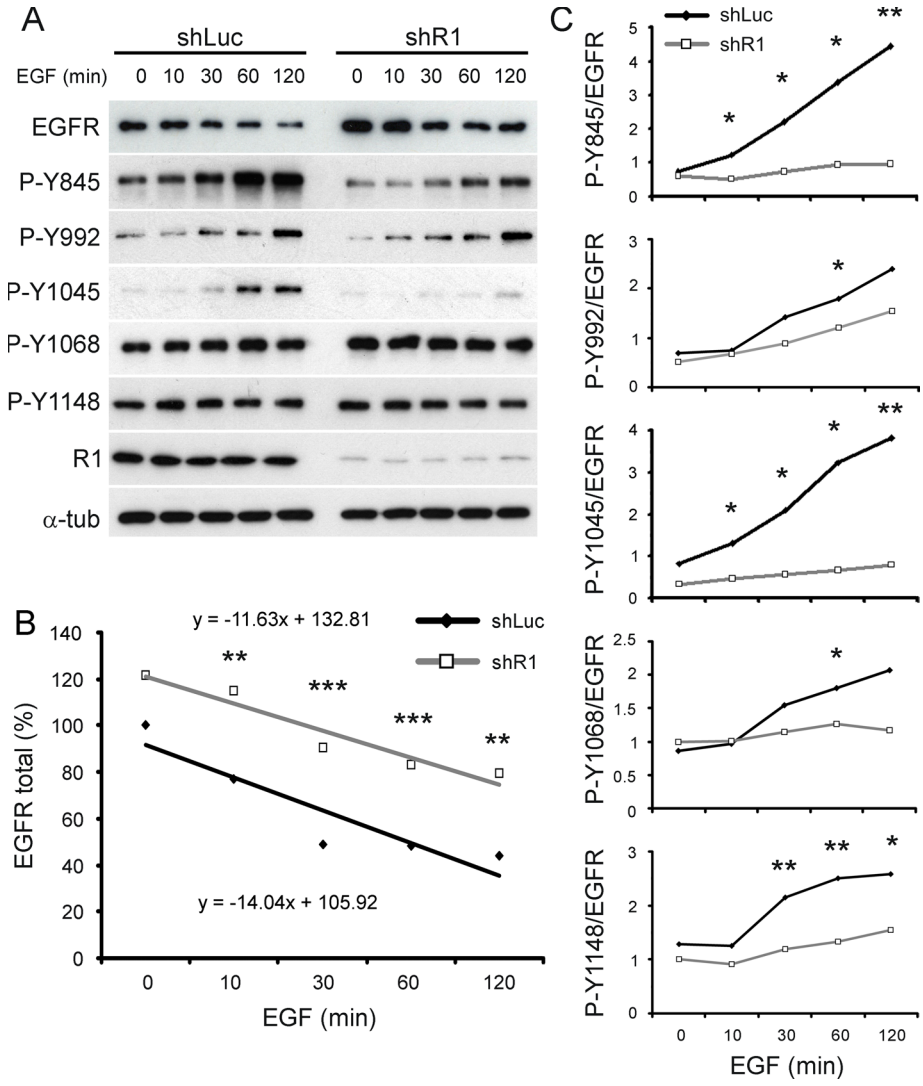

FIGURE 5: Biochemical analysis of EGFR phosphorylation. (A–C) Control shLuc and shR1 cells were exposed to 10 ng/ml EGF between 0 and 120 min, and the total EGFR and the phosphorylation (P) of specific tyrosine residues of EGFR were determined with specific antibodies as indicated. Reggie-1 (R1) and α-tubulin (α-tub) served as loading control. The quantification of the differences between shLuc and shR1 cells of total EGFR as well as each of the five tyrosine residues normalized to total EGFR are shown in B and C, respectively (n = 4, *p < 0.05, **p < 0.01, ***p < 0.001, paired *t* test).

Rescue of AJ formation

As mentioned, E-cadherin is internalized by macropinocytosis and recycled at steady state (Bryant *et al.*, 2007). This observation, together with our finding that down-regulation of reggies raises the rate of macropinocytosis and disturbs AJ formation and dynamics, led to the hypothesis that these phenomena are causally linked. Thus blockage of macropinocytosis in shR1 cells might counterbalance the abnormal AJ phenotype. Therefore we monitored AJ formation in E-cadherin-EGFP–expressing shR1 cells after amiloride treatment, a classic blocker of macropinocytosis (Kerr and Teasdale, 2009). As expected, amiloride blocked the increased uptake of dextran in shR1 cells after EGF stimulation (Supplemental Figure S6, C and D). Of importance, AJ formation, which is severely disturbed in shR1 cells (Figure 3C), returned to near-normal rates upon amiloride treatment (Figure 8A and Table 2). It has been reported that amiloride, by affecting the pH in the endocytic structures, blocks Rac1 (Koivusalo *et al.*, 2010). Therefore we tested directly whether a specific Rac1 inhibitor had the same rescuing effect as amiloride. Indeed, the Rac1 inhibitor increased AJ formation in shR1 cells (Figure 8B and Table 2). Because down-regulation of reggies induced higher levels of p38 kinase activation after EGF stimulation (Figure 6), we used a p38-specific inhibitor and rescued the defects in AJ formation (Table 2). On the other hand, no rescue effects were observed with inhibitors of other EGFR downstream signaling molecules, such as MEK1/2, PLC, and ROCK (Figure 8C and Table 2). Thus the EGFR signaling involved in macropinocytosis affects the reggie-dependent regulation of AJs.

Consistent with the well-characterized role of PI3K in the regulation of macropinocytosis in EGF-stimulated A431 cells (Araki *et al.*, 2007), the AJ phenotype of shR1 cells was also rescued by a PI3K-specific inhibitor (Figure 8D and Table 2). This result appears incongruent with the reduced phosphorylation of the PI3K-regulatory subunits p85 and p55 observed in shR1 cells during EGF stimulation (Figure 6). However, the reduced PI3K activation is in agreement with the reduced downstream activation of Akt (Figure 6), since both kinases seems to require EGFR signaling in endosomes to complete activation (Murphy *et al.*, 2009). To reconcile this issue, we analyzed the role of PI3K and Akt in the EGF-mediated macropinocytosis of shR1 cells using specific inhibitors. Indeed, the PI3K inhibitor blocked the increased uptake of dextran in shR1 cells after EGF stimulation, whereas the Akt inhibitors IV and VIII had no significant effects (Supplemental Figure S6, E and F). Together these results indicate that the EGF-mediated PI3K activation, but not its downstream signaling to Akt, is involved in the increased macropinocytosis of shR1 cells. Because the first step in the activation of PI3K is believed to occur at the PM (Sorkin and von Zastrow, 2009), we speculate that the delayed EGFR endocytosis in shR1 cells might induce a local increase in the PI3K activity at the cell surface. Therefore we analyzed the subcellular localization of the phosphorylated PI3K subunits p85 and p55 in shR1 and control shLuc cells during EGF stimulation. Immunostainings revealed a weak signal for the activated PI3K subunits in serum-starved cells, which clearly increased upon EGF stimulation (Figure 8E), confirming the specificity of the antibody. Of interest, we observed an accumulation of the phosphorylated PI3K subunits at the apical pole of cell contacts after 20 min of EGF treatment in shR1 cells (Figure 8E). Conversely, EGF-stimulated shLuc cells displayed more widespread signals of the activated PI3K subunits at the apical and basal regions without accumulation at cell contacts (Figure 8E). In sum, our results indicate that AJ formation is impaired in shR1 cells because the delayed EGFR internalization enhances its signaling at the PM (probably at the apical region), which, in turn, increases macropinocytosis and recycling of E-cadherin to AJs.

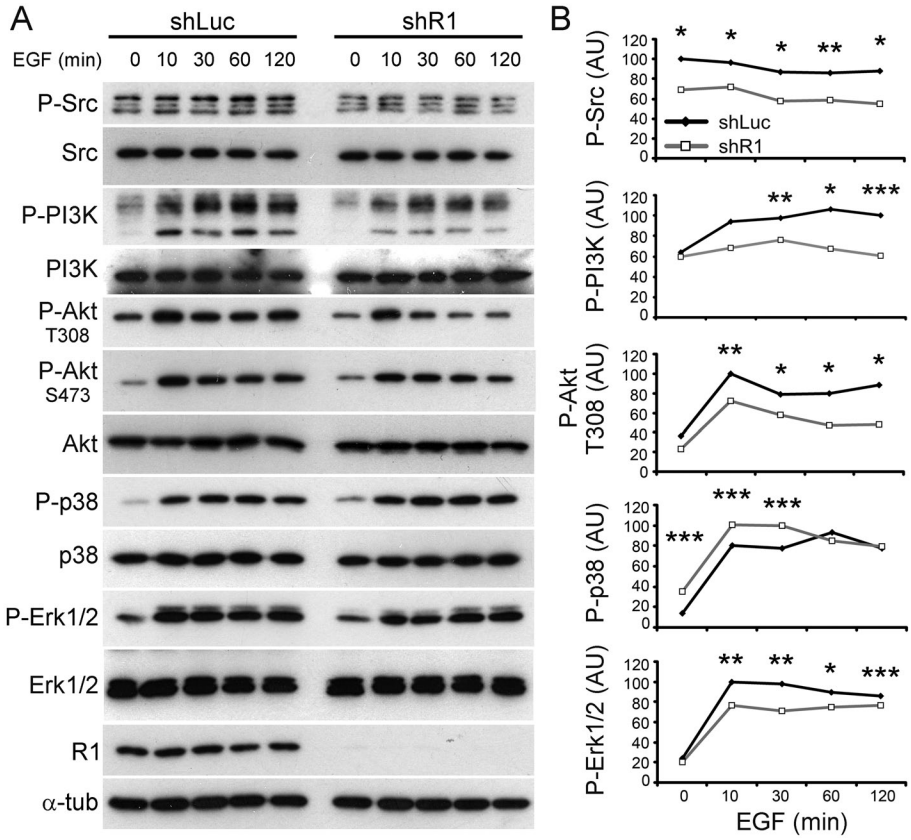

FIGURE 6: Biochemical analysis of EGFR downstream targets. (A) shLuc and shR1 cells were stimulated with EGF as indicated in Figure 5. Western blot analyses show that the phosphorylation (P) of Src, PI3K subunits p85 and p55, Akt (T308 and S473), p38, and Erk1/2 kinases is altered in shR1 cells. Antibodies against total Src, PI3K subunit p85, Akt, p38, Erk1/2, reggie-1 (R1), and α-tubulin (α-tub) were used as loading control. (B) Quantification of the differences between shLuc and shR1 cells from A (n = 4, *p < 0.05, **p < 0 .01, **p < 0.001, paired *t* test).

To obtain a first impression of whether this hypothesis holds true, we monitored E-cadherin-EGFP–labeled vesicles within EGF-stimulated shR1 and control shLuc cells. E-cadherin–positive vesicles were tracked and quantified at the focal plane of newly forming AJs (basal pole of cell contacts; Hong *et al*., 2010). Indeed, the amount of E-cadherin–positive vesicles traveling in the basal region of cell contacts was significantly increased in shR1 cells compared with shLuc cells (Figure 8, F and G, and Supplemental Movies S4 and S5). This result shows that down-regulation of reggies results in an increase in E-cadherin vesicle trafficking during EGF stimulation. Finally, we analyzed whether reggies might be involved in the targeting of E-cadherin–loaded vesicles to AJs. EGF treatment of A431 cells cotransfected with E-cadherin–EGFP and reggie-1–monomeric red fluorescent protein (mRFP) showed the expected colocalization of both proteins in macropinosomes (Figure 8H). In addition, we observed double-labeled vesicles and vesiculotubular structures (Figure 8H). Then we recorded vesicle trafficking at the focal plane of the AJs upon EGF stimulation. The vast majority of vesicles carried both E-cadherin and reggie-1 (Supplemental Figure S6G). Of importance, double-labeled vesicles and highly dynamic vesiculotubular structures were observed to move toward as well as from AJs (Supplemental Figure S6G and Supplemental Movie S6). These data suggest that reggies may be involved in the trafficking of E-cadherin and its targeted delivery to AJs.

	Inhibitor	Number of AJs (AJ/μm²)
shLuc		0.170 ± 0.014
shR1		0.043 ± 0.009***
shR1	+ amiloride	0.157 ± 0.020
shR1	+ Rac1	0.132 ± 0.006
shR1	+ PI3K	0.168 ± 0.018
shR1	+ p38	0.165 ± 0.018
shR1	+ MEK1/2	0.064 ± 0.007***
shR1	+ PLC	0.034 ± 0.004***
shR1	+ ROCK	0.043 ± 0.006***

The macropinocytosis blocker amiloride rescued the AJ formation defects (number of AJs) in shR1 cells. Blockers of Rac1, PI3K, and p38 increased the formation of AJs, whereas this effect was not observed by the inhibitors of MEK1/2, PLC, and ROCK. Statistical differences related to shLuc cells. n = 3, ***p < 0.001, one-way ANOVA, mean ± SEM.

TABLE 2: Macropinocytosis blockers rescue AJ formation.

DISCUSSION

The results of this study show that down-regulation of reggies and PrP impaired cell adhesion by disrupting the spatiotemporal pattern of AJs, which normally undergo a basal-to-apical flow at the cell contact sites: AJs stalled or failed to form in shR1 and shPrP cells. Dissection of the underlying events uncovered that down-regulation of reggies led on the one hand to the reduction of activated Src tyrosine kinases and of phosphorylation of the tyrosine residue (Y805) on EGFR, which is the target of Src, and on the other hand had a major effect on tyrosine phosphorylation of the EGFR residue (Y1045) relevant for c-cbl–dependent EGFR internalization (Sorkin and Goh, 2008). Delayed internalization prolonged EGFR signaling at the PM, and this, in turn, increased the efficacy of E-cadherin macropinocytosis and negatively affected AJ formation (Figure 9). Indeed, AJ malformation correlated with and probably arose from defects in the trafficking of E-cadherin vesicles at the level of the AJs in shR1 cells. Thus reggies apparently coordinate the trafficking of specific cargo vesicles involved in membrane protein recycling and redelivery in epithelial cells.

Reggies, Src tyrosine kinase, and c-cbl

The two effects of reggies (regulation of Src activity and c-cbl–dependent events) are in line with earlier evidence showing that reggies interact with several Src tyrosine kinases in many different cells (Stuermer, 2010) and that reggies communicate with c-cbl through CAP (c-cbl–associated protein; Kioka *et al*., 2002). The functional association between EGFR and Src might connect EGFR to PrP- and reggie-mediated signaling, since both reggie and PrP

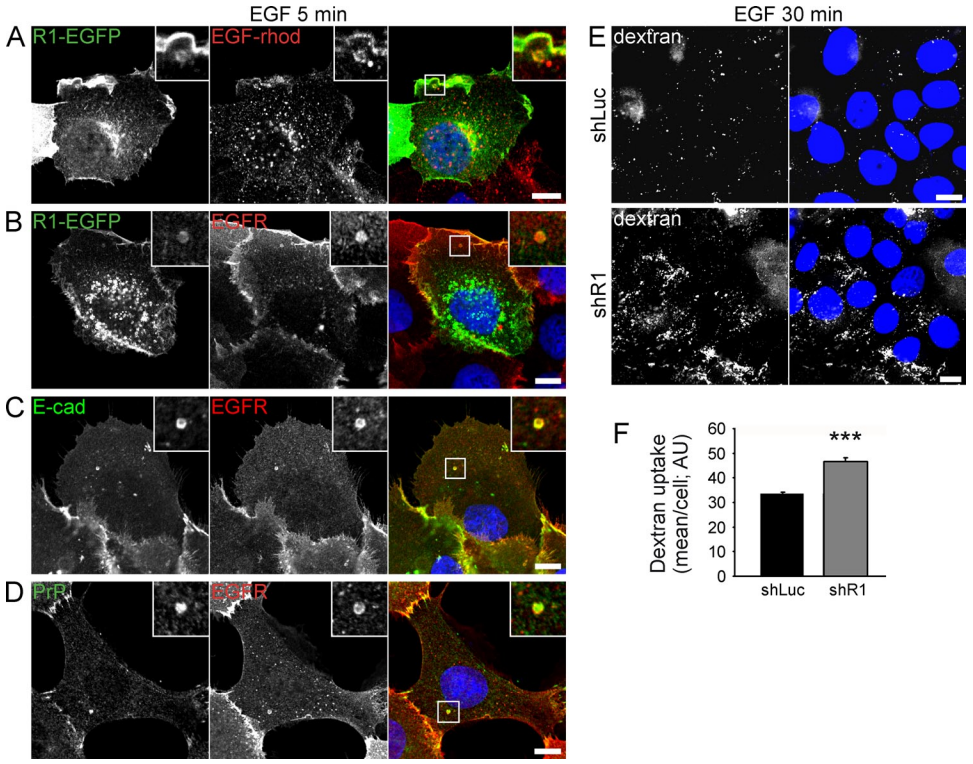

FIGURE 7: Formation of macropinosomes in A431 cells treated with EGF. (A) Reggie-1-EGFP (R1-EGFP)–transfected cells showed colocalization of reggie-1 and EGF-rhodamine (EGF-rhod) in the forming macropinosome after 5 min of EGF treatment (boxed area enlarged in inserts). (B) R1-EGFP colocalized with EGFR in a macropinosome. (C, D) Immunostaining with antibodies against E-cadherin (E-cad) and EGFR, as well as with antibodies against PrP and EGFR, showed colocalization of the protein pairs in macropinosomes. Scale bars, 10 μm. (E, F) Addition of Alexa-dextran (dextran) showed a significantly higher amount of internalization in shR1 cells compared with control shLuc cells (n = 3, ***$p < 0.001$, *t* test, mean ± SEM). Scale bars, 10 μm.

associate with and trigger signals via Src-family tyrosine kinases (Stuermer, 2010). Our results are in agreement with the view that PrP *trans*-interactions in reggie microdomains activate Src kinases (Solis *et al.*, 2010; Stuermer, 2010), thereby affecting EGFR phosphorylation and endocytosis. This might explain previous results showing that Erk1/2 activation induced by antibody cross-linking of PrP is mediated by EGFR signaling (Monnet *et al.*, 2004) and that Src kinase activity increases EGFR endocytosis during EGF stimulation (Ware *et al.*, 1997). Furthermore, our results suggest that the activity of c-cbl, which is crucial for EGFR down-regulation (Sorkin and Goh, 2008), depends on reggies. c-cbl has been involved in the regulation of a reggie-dependent signaling cascade leading to the activation of the small GTPase TC10 (Kioka *et al.*, 2002) and in the targeted recycling of specific cell surface receptors (Baldys *et al.*, 2009). This suggests a function of the reggie/c-cbl interaction in guiding E-cadherin to the forming AJs.

Reggies and macropinocytosis

Our results indicate that the prolonged surface exposure of EGFR in shR1 cells influences EGFR signaling and the ensuing activation at the PM of PI3K and Rac1, which, in turn, regulate macropinocytosis (Kerr and Teasdale, 2009). Thus, through their effect on EGFR phosphorylation and internalization, reggies restrict the efficacy of macropinocytosis. The fact that macropinocytosis was increased in the absence of reggies implies that they are not required for processes such as formation of the macropinocytic cup or its budding into the cell. Reggies assembled at macropinocytic structures containing E-cadherin, EGFR, and PrP and, according to live observations, might control the trafficking of E-cadherin vesicles at the level of AJs. Thus reggies seem to guarantee a well-controlled macropinocytic uptake of E-cadherin (and EGFR) and the targeted recycling of E-cadherin (and probably a fraction of EGFR) to the forming AJs. We observed that the total amount of E-cadherin at the PM versus intracellular compartments was unchanged in shR1 and shPrP cells. This is expected if macropinocytic uptake of E-cadherin is counterbalanced by its recycling back to the PM, as previously reported (Bryant *et al.*, 2007).

We observed that the tyrosine phosphorylation level of β-catenin was increased in our shR1 and shPrP cells without an apparent effect on E-cadherin/catenin complex formation. Phosphorylation of β-catenin by EGFR, Src, and various other kinases is believed to negatively affect E-cadherin/catenin interactions and adhesion (Lilien and Balsamo, 2005). This view, however, has been challenged in an elegant paper using β-catenin/plakoglobin double-null F9 cells (Tominaga *et al.*, 2008). That study uncovered the phosphorylation of various tyrosine residues that had no effect on E-cadherin/catenin complex formation and cell adhesion. The identification of the tyrosine residue(s) responsible for the increased β-catenin phosphorylation in our shR1 and shPrP cells and its/their potential role in E-cadherin macropinocytosis await further analysis.

The role of PrP in E-cadherin turnover and recruitment

Aside from the fact that reggie depletion led to down-regulation of PrP, cells in which only PrP was down-regulated mimicked the reggie phenotype in several respects. That PrP colocalized with reggies, E-cadherin, and EGFR not only at cell contact sites, but also in the macropinosomes, suggests that PrP might be functionally involved

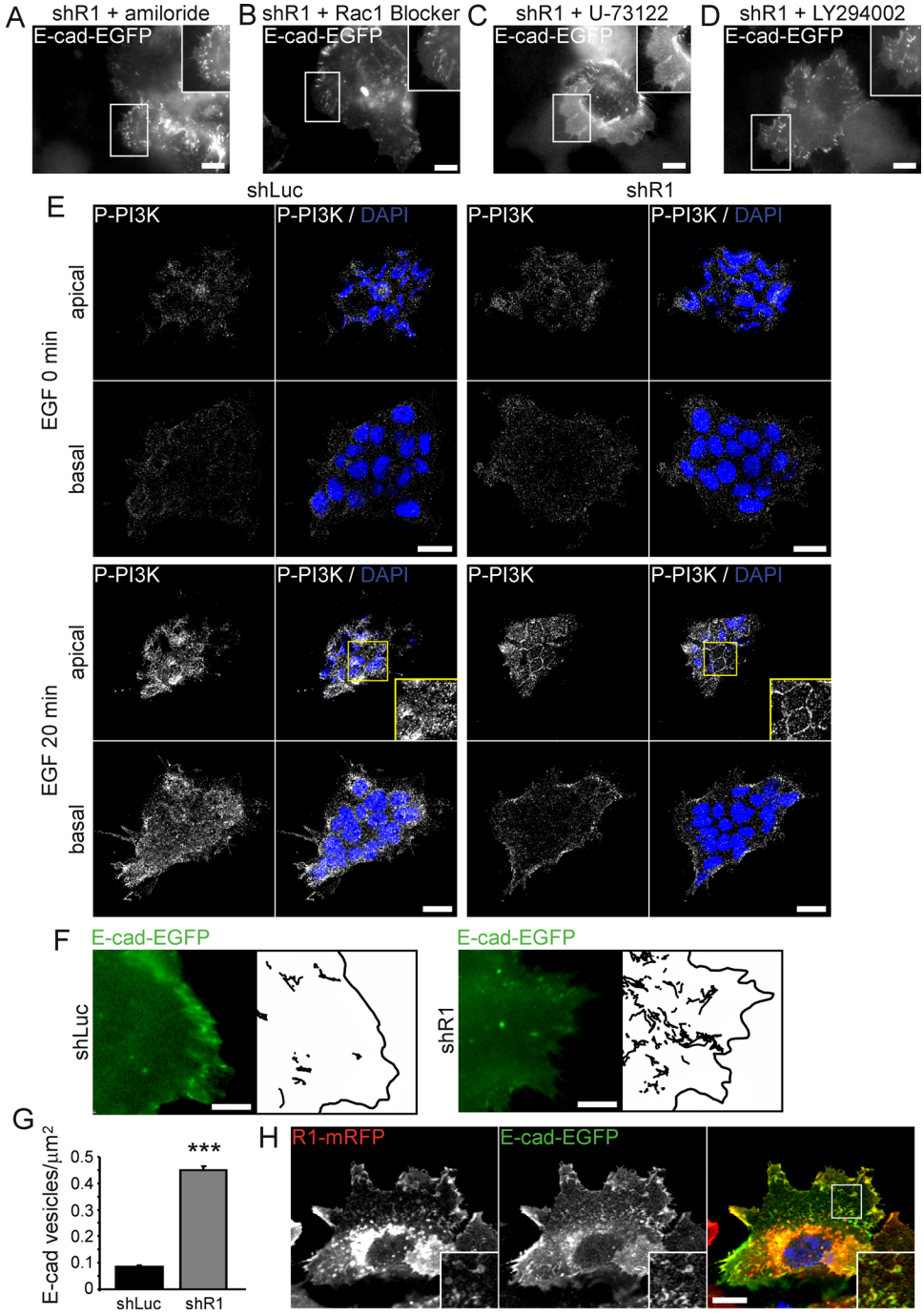

FIGURE 8: Macropinocytosis blockers rescue AJ formation in reggie-knockdown cells. (A–D) E-cadherin-EGFP (E-cad-EGFP)–transfected shR1 cells showed a recovery of AJ formation when treated with the macropinocytosis blockers amiloride (A), Rac1 (B), and PI3K (LY294002, D) but not when treated with the PLC blocker U-73122 (C). Selected areas showed cell contacts between E-cad–EGFP expressing and nontransfected cells for better visualization. Scale bars, 5 µm. (E) shLuc and shR1 cells were either nonstimulated (EGF 0 min) or stimulated with 10 ng/ml EGF for 20 min and immunostained with an antibody against the phosphorylated PI3K subunits p85 and p55 (P-PI3K). The weak staining of nonstimulated cells contrasts with the stronger signals after EGF stimulation, particularly in shLuc cells. Phosphorylated PI3K subunits accumulated at cell contacts in the apical pole of shR1 cells (boxed area), as opposed to a more widespread distribution in shLuc cells at apical and basal regions. Scale bars, 20 µm. (F) E-cad-EGFP–labeled vesicles of EGF-stimulated control shLuc and shR1 cells were monitored by time-lapse recordings at the focal plane of AJs for 1 min. The vesicle tracks were traced as indicated by the lines (right). Scale bars, 5 µm. (G) The quantification of E-cadherin vesicles emerging into the focal plane of AJs showed a significant increase in shR1 over control shLuc cells (n = 10, ***$p < 0.001$, *t* test, mean ± SEM). (H) E-cad-EGFP– and reggie-1-mRFP (R1-mRFP)– cotransfected A431 cells were stimulated with EGF for 15 min. A selected frame (boxed areas) showed that both proteins were colocalized at the same vesicles and tubulovesicular structures. Scale bars: 10 µm.

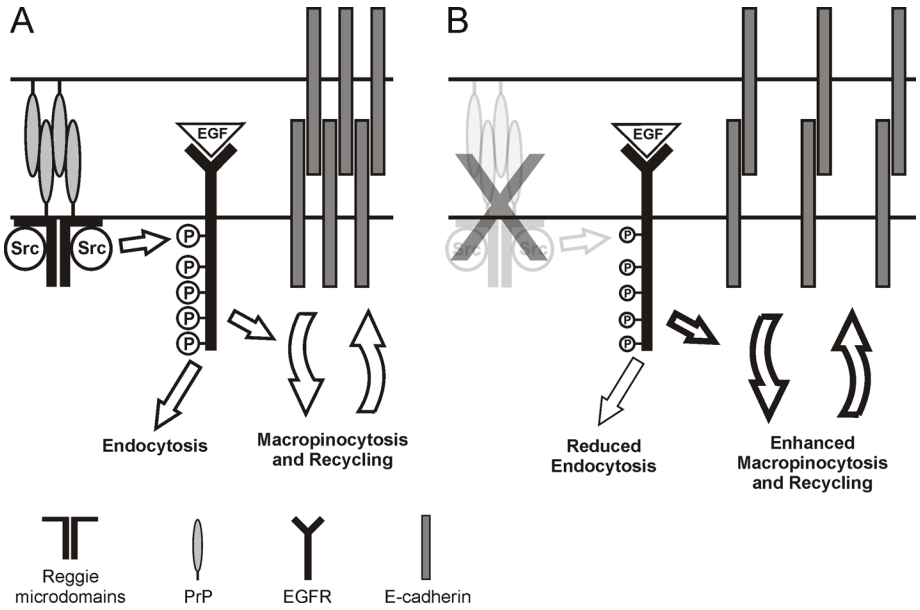

FIGURE 9: Model of the role of reggies and PrP in AJ formation. (A) In epithelial cells, PrP homophilic *trans*-interactions trigger clustering of PrP in reggie microdomains and activate Src-family tyrosine kinases at cell–cell contacts. This activated pool of Src kinases seems to be necessary for the correct phosphorylation of the Y845 residue of the EGFR during EGF stimulation. In addition, Y845 phosphorylation might be required for the proper autophosphorylation of various other tyrosine residues of the receptor, especially the Y1045 residue, which is known to be associated with the c-cbl–dependent EGFR internalization. EGF stimulation of EGFR at the PM, in turn, triggers the macropinocytosis of E-cadherin from AJs, which is recycled back to the cell contacts sites for the formation of new AJs. (B) The down-regulation of reggies or PrP generates a decrease in Src activation and an overall reduction in EGFR tyrosine phosphorylation during EGF stimulation. This impairs EGFR endocytosis, leading to the retention of the receptor at the PM and to the reduction in the activation of downstream molecules known to require EGFR-signaling endosomes. The increased surface EGFR signaling causes an enhanced macropinocytosis of E-cadherin from AJs. Thus the accelerated macropinocytosis and subsequent recycling of E-cadherin negatively affects the formation of AJs.

in the macropinocytic uptake and recycling of E-cadherin to AJs. The detailed analysis of PrP's affect on the generation of AJs awaits further experimentation. However, the contribution of PrP to these events might consist in the recruitment of E-cadherin from the vesicles to cell contacts as in the zebrafish embryo (Malaga-Trillo *et al.*, 2009). In the embryo, recruitment of E-cadherin to contact sites required PrP *trans*-interactions and might be needed for the recruitment of E-cadherin from macropinocytic vesicles back to AJs. PrP may exert this function by interacting with reggies and its associated signaling molecules. Together they could form a landmark for E-cadherin deployment in epithelial cells (Stuermer, 2010).

Reggies and clathrin-mediated endocytosis

We showed here that EGFR phosphorylation and internalization are impaired in shR1 cells. However, we did not directly examine which routes EGFR takes into the cells. The fact that we did not observe reggie-1 at EGF-rhodamine vesicles other than macropinosomes suggests that reggies are not directly (physically) involved in EGFR endocytosis. The clathrin-coated pit pathway is perhaps the most important pathway of EGFR internalization (Sorkin and Goh, 2008). This would imply that reggies facilitate the clathrin-mediated endocytosis of EGFR. Accordingly, it was recently demonstrated that reggies can modulate the clathrin-dependent uptake of the amyloid precursor protein (Schneider *et al.*, 2008), the dopamine transporter (Cremona *et al.*, 2011), and a cholesterol transporter (Ge *et al.*, 2011). The modulation of the clathrin-dependent endocytosis via reggies might involve an interaction with the adapter AP2 (Ge *et al.*, 2011), although reggies were previously not observed at clathrin-coated pits (Langhorst *et al.*, 2008; Schneider *et al.*, 2008).

During the revision of this paper, an article was published showing that siRNA-mediated down-regulation of reggie-2 in HeLa cells reduced the EGF-mediated phosphorylation of EGFR (only at Y1173) and Erk1/2 but had no effect on EGFR endocytosis and the PI3K/Akt pathway (Amaddii *et al.*, 2012). Our results, however, show that reggie-1 down-regulation inhibits EGFR phosphorylation at various residues (particularly at Y845 and Y1045), impairs EGFR endocytosis and degradation, and affects the downstream targets PI3K/Akt and Erk1/2, which are known to require receptor endocytosis (Murphy *et al.*, 2009; Sorkin and von Zastrow, 2009). Thus the different effects on the EGFR pathway induced by siRNAs against reggie-2 might result from the high residual levels of reggie-1 observed under these conditions (Amaddii *et al.*, 2012).

Reggies drive macropinocytic membrane turnover and redelivery

Our work on EGFR indicates that its internalization is impaired in shR1 cells. This enhances the macropinocytosis through which E-cadherin is redelivered to cell contact sites. Yet redelivery might be imprecise in shR1 cells, which correlates with increased and, by inference, error-prone E-cadherin vesicle trafficking. The latter role of reggies—macropinocytic recycling and targeted redelivery of the macropinocytic cargo—could explain results from other reports and indicates which function reggies might generally subserve. For example, in neurons reggies are enriched in the growth cone and are indispensable for axon elongation (Stuermer, 2010). In addition, reggies were implicated in the turnover of semaphorins in the growth cone (Carcea *et al.*, 2010). This fits the notion that neurons use a highly efficient macropinocytic turnover mechanism of membrane and associated proteins during growth cone elongation and navigation (Tojima *et al.*, 2011). This mechanism is known to be regulated by neurotrophin receptor tyrosine kinases (Valdez *et al.*, 2007). Of interest, neutrophils derived from a reggie-2/flotillin-1 knockout mouse had problems with chemotactic movements in Matrigel, which correlates with the accumulation of reggies at the uropod of these cells (Ludwig *et al.*, 2010). Migratory cells depend, like growth cones, on macropinocytic membrane turnover at their leading and trailing edges, and migration is also triggered by stimulation of receptor tyrosine kinases.

Thus, if reggies generally regulate the macropinocytic turnover mediated by receptor tyrosine kinases in polarized cells, this would account for the fact that reggies are present in virtually every cell type and why they have been implicated in seemingly different functions.

MATERIALS AND METHODS

Reagents, antibodies, and plasmids

Cell culture reagents were purchased from Life Technologies (Darmstadt, Germany). Antibodies and their distributors were as

follows: monoclonal antibodies (mAbs) against E-cadherin, p120, β-catenin, α-catenin, ESA/reggie-1, flotillin-1/reggie-2, EGFR, and caveolin-1 (BD Biosciences, Heidelberg, Germany); anti-PrP (6H4; Prionics, Schlieren-Switzerland, Zurich, Switzerland); desmoplakin 1/2 (Progen, Heidelberg, Germany); mAb against phosphotyrosine (PTyr100) and the polyclonal antibodies (pAbs) against E-cadherin, EGFR, c-cbl, phospho-EGFR Y845, Y992, Y1045, Y1068, and Y1148, Src, phospho-Src Y416, Akt, phospho-Akt Thr-308, phospho-Akt Ser-473, p38, phospho-p38 Thr-180/Tyr-182, PI3K p85, phospho-PI3K (p85 Y458/p55 Y199), Erk1/2, and phospho-Erk1/2 Thr-202/204 (Cell Signaling, Frankfurt am Main, Germany); and pAb anti–α-tubulin (Abcam, Cambridge, MA). Secondary antibodies for immunostaining and Western blot analyses were from Jackson ImmunoResearch Laboratories (West Grove, PA). Phalloidin–Alexa 548 was from Invitrogen (Carlsbad, CA). The following inhibitors were used: EGFR inhibitors PD158780 (Sigma-Aldrich, St. Louis, MO) and tyrphostin AG-1478 (Cell Signaling); PI3K inhibitor LY294002 and MEK1/2 inhibitor U0126 (Cell Signaling); Rac1-inhibitor and Akt inhibitors IV and VIII (Calbiochem, La Jolla, CA); and amiloride, p38 kinase inhibitor SB 202190, PLC inhibitor U-73122, and ROCK inhibitor Y-27632 (Sigma-Aldrich). The reggie-1–EGFP rescue construct and the caveolin-1–EGFP vector were described previously (Langhorst *et al.*, 2008; Munderloh *et al.*, 2009). The human E-cadherin–EGFP vector was generously provided by Vann Bennett (Duke University Medical Center, Durham, NC).

Cell culture and cell lines

A431, MCF-7, and HeLa cells were cultured in DMEM supplemented with 10% fetal calf serum, L-glutamine, and penicillin/streptomycin. A431 cells were growth until ~90% of confluency (hereafter indicated as "near confluency") to avoid the formation of multiple cell layers (Van Itallie *et al.*, 1995). Vector transfection was carried out using FugeneHD (Roche, Mannheim, Germany), following the manufacturer's protocol, and siRNA transfection using Nanofectin siRNA transfection reagent (PAA, Linz, Austria). Alexa Fluor 546–labeled siRNA duplexes against reggie-1 (R1.0) and PrP were obtained from Qiagen (Valencia, CA), and the target sequences were previously described (Solis *et al.*, 2007; Schrock *et al.*, 2009).

Permanent reggie-1 and PrP depletion in A431 cells was obtained by shRNA interference with annealed primers expressed in the pRetroSuper vector (kindly provided by Dietmar Schreiner, University of Iowa, Iowa City, IA). Primers used for reggie-1 are as follows: 5′ sense strand, 5′-gatccccGGTGAAGATCATGACGGAGttcaagagaCTCCGTCATGATCTTCACCttttta-3′, and 3′ antisense strand, 5′-agcttaaaaaGGTGAAGATCATGACGGAGtctcttgaaCTCCGTCATGATCTTCACCggg-3′. For PrP they are as follows: PrPA 5′ sense strand, 5′-gatccccCCGGATAGGCTAATCAATAttcaagagaTATTGATTAGCCTATCCGGttttta-3′, and 3′ antisense strand, 5′-gcttaaaaaCCGGATAGGCTAATCAATAtctcttgaaTATTGATTAGCCTATCCGGggg-3′; PrPB 5′ sense strand, 5′-gatccccGTGACTATGAGGACCGTTAttcaagagaTAACGGTCCTCATAGTCACttttta-3′, and 3′ antisense strand, 5′-agcttaaaaaGTGACTATGAGGACCGTTAtctcttgaaTAACGGTCCTCATAGTCACggg-3′. shLuc control vector expressing a shRNA against firefly luciferase was provided by Dietmar Schreiner. Annealed primers were cloned using the *Bam*HI and *Hin*dIII sites of the pRetroSuper vector. To generate stable knockdown lines, shRNA vectors were transfected into A431 cells and cells cultured under selection in 10 µg/ml puromycin.

E-cadherin-EGFP–expressing A431 cells were generated by transfection with the E-cadherin-EGFP and by selection in 0.8 mg/ml G418.

Immunofluorescence and microscopy

A431, MCF-7, and HeLa cells were fixed and stained as previously described (Langhorst *et al.*, 2008). Cells were analyzed with an α-Plan-Apochromat 63×/1.4 objective at a confocal microscope (LSM510 Meta) and/or Axioplan2 equipped with an AxioCam HRm (all from Zeiss, Jena, Germany).

Visualization of Triton-resistant AJs in A431 cell lines was performed according to Shewan *et al.* (2005). Briefly, cells were grown on poly-L-lysine (pLys)–coated coverslips to near confluency, immersed for 10 s in ice-cold Triton buffer (10 mM 4-(2-hydroxyethyl)-1-piperazineethanesulfonic acid [HEPES], pH 7.4, 50 mM NaCl, 3 mM $MgCl_2$, 300 mM sucrose, 0.2% Triton X-100), fixed, and immunostained as described.

Quantification of overlapping cell contacts

A431 cell lines were grown on pLys-coated coverslips until near confluency, fixed, and stained for E-cadherin and 4′,6-diamidino-2-phenylindole. Widefield images were acquired in an Axioplan2 microscope, and the overlapping area of ~400 cell contacts was marked and measured using AxioVision 4.8 software (Zeiss). The mean area covered by cell contacts of shRNA control cells was set to 100%, and statistical analysis was performed from three independent experiments using a one-way analysis of variance (ANOVA) test.

Dispase-based dissociation assay

The dispase-based dissociation assay has been previously described (Huen *et al.*, 2002). Briefly, shRNA stably transfected A431 cells were grown in duplicate on 60-mm plates until confluency was entirely reached. Cells were washed with PBS and incubated with a 2.4 U/ml dispase (Roche) solution for 1 h at 37°C, and the released cell carpets were carefully washed and transferred to 15-ml tubes. Tubes were inverted 60 times on a rocker, and cell fragments were counted. Quantification was done from four replicates of three independent experiments and statistical analyses using a one-way ANOVA test.

Scratch assay

A431 cells were grown to near confluency on a 12-well plate, and a scratch was performed with a tip of a micropipette. Cells were washed twice with PBS and cultured normally. Images of the wound were taken after indicated time points and the empty (wound) area was measured. The percentage of wound closure was calculated by comparing the initial wound area with the wound after 24 h. Quantification was done from four replicates of three independent experiments and statistical analyses using a paired *t* test.

Electron microscopy analyses

Electron micrographs taken randomly at 20,000 primary magnification were enlarged to 80,000 times for morphometric analyses of AJs. The apparent length of structures fulfilling the criteria of AJs in A431 cells, as exemplified by Troyanovsky *et al.* (2006), was measured where they occurred in strictly perpendicular section.

Biochemical analyses

A431 cells grown on plates to near confluency were lysed with ice-cold lysis buffer (20 mM Tris-HCl, pH 7.5 100 mM NaCl, 5 mM $MgCl_2$, 2 mM EDTA, 1% Triton X-100, 10% glycerin) supplemented with protease and phosphatase inhibitor cocktails (ThermoFisher Scientific, Waltham, MA). Extracts were cleared by centrifugation and boiled at 95°C for 5 min or used for coimmunoprecipitation analyses. Briefly, lysates were incubated with 1 µg of antibody against E-cadherin, p120, or β-catenin for 1 h at 4°C. Then 20 µl of protein G agarose (Roche) was added and incubated overnight at

4°C. The beads were washed and prepared for SDS–PAGE and Western blots. Lipid rafts were isolated as described previously (Stuermer *et al.*, 2004). Quantification of blots was done using ImageJ (National Institutes of Health, Bethesda, MD).

Quantification of cell surface E-cadherin and E-cadherin endocytosis

shRNA permanently transfected A431 cells grown on plates to near confluency were incubated on ice with 1 mg/ml sulfo-NHS-SS-biotin (Pierce, ThermoFisher Scientific) in PBS for 30 min. Free sulfo-NHS-SS-biotin was quenched by two washes with ice-cold 50 mM NH_4Cl in PBS containing 1 mM $MgCl_2$ and 0.1 mM $CaCl_2$ and several washes in PBS. Cell extracts and E-cadherin immunoprecipitation were done as described. Biotinylated E-cadherin was analyzed by Western blots using ExtrAvidin-peroxidase (Sigma-Aldrich) and anti–E-cadherin mAb.

For E-cadherin trypsinization, A431 cells were grown on plates to near confluency and incubated in HEPES-buffered saline supplemented with 0.01% trypsin for 10 min at 37°C in the presence of 2 mM Ca^{2+} or 1 mM ethylene glycol tetraacetic acid. Cells were immediately boiled in Laemmli buffer, and E-cadherin was detected by Western blots.

Endocytosis of E-cadherin was studied as previously described (Le *et al.*, 1999). Briefly, A431 cells grown on plates to near confluency were biotinylated as described. Cells were incubated for 2 h at 37°C in normal media supplemented with 10 μM cycloheximide to stop protein synthesis. Surface biotin was removed by incubation with three 20-min washes with ice-cold glutathione solution (60 mM glutathione, 75 mM NaCl, 75 mM NaOH, and 1% bovine serum albumin). Biotinylated proteins from cleared cell extracts (lysed as described earlier) were collected with 10 μl of streptavidin beads overnight at 4°C and finally analyzed by Western blot against E-cadherin.

EGF stimulation

Transfected and nontransfected shRNA A431 cells were serum starved for 4 h, stimulated with 10 ng/ml EGF (Sigma-Aldrich) in DMEM-HEPES, pH 7.4, supplemented with 10 μM cycloheximide for the time indicated in the corresponding figures, and prepared for immunostaining, biotinylation, and biochemical analyses as described. Statistical analyses were done using a one-way ANOVA test or a paired *t* test from at least three independent experiments.

EGF-rhodamine and dextran uptake

A431 cells were prepared as described, stimulated with 20 ng/ml EGF-rhodamine (Molecular Probes, Invitrogen) or with 10 ng/ml EGF in the presence of 0.5 mg/ml dextran–Alexa Fluor 488 (10,000 MW; Molecular Probes, Invitrogen) for the times indicated in the corresponding figures, fixed, and mounted for confocal microscopy analysis. For EGF-rhodamine uptake, cells were washed three times with ice-cold acidic buffer (0.2 M acetic acid, 0.5 M NaCl) to remove surface-bound EGF-rhodamine before fixation. For dextran uptake experiments, cells were alternatively pretreated for 30 min with dimethyl sulfoxide, 1 mM amiloride, 50 μM LY294002, 1 μM Akt inhibitor IV, or 10 μM Akt inhibitor VIII before EGF stimulation. The LSM Image Browser (Zeiss) was used for fluorescence quantification of ~300 cells per each time point from at least three independent experiments. Statistical analyses were done using a one-way ANOVA test or a paired *t* test.

Live-cell imaging

A431 cells were transfected for 48–72 h on pLys-coated coverslips. Cells were recorded using a Colibri Cell Observer SD imaging system equipped with an α-Plan Fluar 100×/1.45 objective and an AxioCam HRm (Zeiss). Cells were maintained in medium on 37°C preheated incubator and objective, and images were acquired with 100% light-emitting diode power. Images for the analysis of AJs in A431 cells expressing E-cadherin–EGFP were acquired every 2 min for 20-min periods as described. Images were further analyzed using ImageJ and AxioVision 4.8 (Zeiss). Total amount of AJs of 10–20 cell contacts and the distance covered by 25 AJs from five randomly selected cell contacts were measured. Alternatively, cells were stimulated with 10 ng/ml EGF or treated with 50 nM PD158780, 100 nM tyrphostin AG-1478, 1 mM amiloride, 50 μM LY294002, 20 μM U0126, 100 μM Rac1-inhibitor, 20 μM SB 202190, 20 μM U-73122, or 20 μM Y-27632 each for 1 h at 37°C before live imaging and analyzed as described. For kymograph analyses, region at the cell contacts were selected, and kymographs were produced using ImageJ; the speed of cell movement was calculated using the plug-in Kymo Line ROI (Elisa May, University of Konstanz). For vesicle trafficking, E-cadherin-EGFP–transfected and R1-mRFP–cotransfected A431 cells were serum starved for 4 h and stimulated with 10 ng/ml EGF during the recording. Images were acquired every 0.5 s for 5 min as described. Cell contacts of 10–20 cells were measured and analyzed using AxioVision 4.8 and Imaris software (Bitplane Scientific Software, Zurich, Switzerland). Statistical analysis was performed using a one-way ANOVA test or a paired *t* test.

ACKNOWLEDGMENTS

We thank Alexander Bledowski for electron microscopy techniques. We are grateful to Alex Räber, Prionics (Zürich, Switzerland), for gifts of the 6H4 mAb against PrP. This work was supported by grants from the Deutsche Forschungsgemeinschaft to C.A.O.S. and H.P.

REFERENCES

Amaddii M, Meister M, Banning A, Tomasovic A, Mooz J, Rajalingam K, Tikkanen R (2012). Flotillin-1/reggie-2 plays a dual role in the activation of receptor tyrosine kinase/map kinase signaling. J Biol Chem 287, 7265–7278.

Araki N, Egami Y, Watanabe Y, Hatae T (2007). Phosphoinositide metabolism during membrane ruffling and macropinosome formation in EGF-stimulated A431 cells. Exp Cell Res 313, 1496–1507.

Baldys A, Gooz M, Morinelli TA, Lee MH, Raymond JR Jr, Luttrell LM, Raymond JR Sr (2009). Essential role of c-Cbl in amphiregulin-induced recycling and signaling of the endogenous epidermal growth factor receptor. Biochemistry 48, 1462–1473.

Bryant DM, Kerr MC, Hammond LA, Joseph SR, Mostov KE, Teasdale RD, Stow JL (2007). EGF induces macropinocytosis and SNX1-modulated recycling of E-cadherin. J Cell Sci 120, 1818–1828.

Carcea I, Ma'ayan A, Mesias R, Sepulveda B, Salton SR, Benson DL (2010). Flotillin-mediated endocytic events dictate cell type-specific responses to semaphorin 3A. J Neurosci 30, 15317–15329.

Cremona ML *et al.* (2011). Flotillin-1 is essential for PKC-triggered endocytosis and membrane microdomain localization of DAT. Nat Neurosci 14, 469–477.

Falcone S, Cocucci E, Podini P, Kirchhausen T, Clementi E, Meldolesi J (2006). Macropinocytosis: regulated coordination of endocytic and exocytic membrane traffic events. J Cell Sci 119, 4758–4769.

Gavard J, Gutkind JS (2008). A molecular crosstalk between E-cadherin and EGFR signaling networks. In: EGFR Signaling Networks in Cancer Therapy, ed. WJ Gullick and JD Haley, Totowa, NJ: Humana Press, 131–146.

Ge L, Qi W, Wang LJ, Miao HH, Qu YX, Li BL, Song BL (2011). Flotillins play an essential role in Niemann-Pick C1-like 1-mediated cholesterol uptake. Proc Natl Acad Sci USA 108, 551–556.

Glebov OO, Bright NA, Nichols BJ (2006). Flotillin-1 defines a clathrin-independent endocytic pathway in mammalian cells. Nat Cell Biol 8, 46–54.

Green KJ, Getsios S, Troyanovsky S, Godsel LM (2010). Intercellular junction assembly, dynamics, and homeostasis. Cold Spring Harb Perspect Biol 2, a000125.

Halbleib JM, Nelson WJ (2006). Cadherins in development: cell adhesion, sorting, and tissue morphogenesis. Genes Dev 20, 3199–3214.
Hong S, Troyanovsky RB, Troyanovsky SM (2010). Spontaneous assembly and active disassembly balance adherens junction homeostasis. Proc Natl Acad Sci USA 107, 3528–3533.
Huen AC *et al.* (2002). Intermediate filament-membrane attachments function synergistically with actin-dependent contacts to regulate intercellular adhesive strength. J Cell Biol 159, 1005–1017.
Kametani Y, Takeichi M (2007). Basal-to-apical cadherin flow at cell junctions. Nat Cell Biol 9, 92–98.
Kerr MC, Teasdale RD (2009). Defining macropinocytosis. Traffic 10, 364–371.
Kioka N, Ueda K, Amachi T (2002). Vinexin, CAP/ponsin, ArgBP2: a novel adaptor protein family regulating cytoskeletal organization and signal transduction. Cell Struct Funct 27, 1–7.
Koivusalo M, Welch C, Hayashi H, Scott CC, Kim M, Alexander T, Touret N, Hahn KM, Grinstein S (2010). Amiloride inhibits macropinocytosis by lowering submembranous pH and preventing Rac1 and Cdc42 signaling. J Cell Biol 188, 547–563.
Langhorst MF, Reuter A, Jaeger FA, Wippich FM, Luxenhofer G, Plattner H, Stuermer CA (2008). Trafficking of the microdomain scaffolding protein reggie-1/flotillin-2. Eur J Cell Biol 87, 211–226.
Le TL, Yap AS, Stow JL (1999). Recycling of E-cadherin: a potential mechanism for regulating cadherin dynamics. J Cell Biol 146, 219–232.
Leu TH, Maa MC (2003). Functional implication of the interaction between EGF receptor and c-Src. Front Biosci 8, s28–s38.
Lilien J, Balsamo J (2005). The regulation of cadherin-mediated adhesion by tyrosine phosphorylation/dephosphorylation of beta-catenin. Curr Opin Cell Biol 17, 459–465.
Ludwig A, Otto GP, Riento K, Hams E, Fallon PG, Nichols BJ (2010). Flotillin microdomains interact with the cortical cytoskeleton to control uropod formation and neutrophil recruitment. J Cell Biol 191, 771–781.
Malaga-Trillo E, Solis GP, Schrock Y, Geiss C, Luncz L, Thomanetz V, Stuermer CA (2009). Regulation of embryonic cell adhesion by the prion protein. PLoS Biol 7, e55.
Monnet C, Gavard J, Mege RM, Sobel A (2004). Clustering of cellular prion protein induces ERK1/2 and stathmin phosphorylation in GT1–7 neuronal cells. FEBS Lett 576, 114–118.
Mosesson Y, Mills GB, Yarden Y (2008). Derailed endocytosis: an emerging feature of cancer. Nat Rev Cancer 8, 835–850.
Munderloh C, Solis GP, Bodrikov V, Jaeger FA, Wiechers M, Malaga-Trillo E, Stuermer CA (2009). Reggies/flotillins regulate retinal axon regeneration in the zebrafish optic nerve and differentiation of hippocampal and N2a neurons. J Neurosci 29, 6607–6615.
Murphy JE, Padilla BE, Hasdemir B, Cottrell GS, Bunnett NW (2009). Endosomes: a legitimate platform for the signaling train. Proc Natl Acad Sci USA 106, 17615–17622.
Nishimura T, Takeichi M (2009). Remodeling of the adherens junctions during morphogenesis. Curr Top Dev Biol 89, 33–54.
Schneider A, Rajendran L, Honsho M, Gralle M, Donnert G, Wouters F, Hell SW, Simons M (2008). Flotillin-dependent clustering of the amyloid precursor protein regulates its endocytosis and amyloidogenic processing in neurons. J Neurosci 28, 2874–2882.
Schrock Y, Solis GP, Stuermer CA (2009). Regulation of focal adhesion formation and filopodia extension by the cellular prion protein (PrPC). FEBS Lett 583, 389–393.
Seveau S, Bierne H, Giroux S, Prevost MC, Cossart P (2004). Role of lipid rafts in E-cadherin– and HGF-R/Met–mediated entry of *Listeria monocytogenes* into host cells. J Cell Biol 166, 743–753.
Shewan AM, Maddugoda M, Kraemer A, Stehbens SJ, Verma S, Kovacs EM, Yap AS (2005). Myosin 2 is a key Rho kinase target necessary for the local concentration of E-cadherin at cell-cell contacts. Mol Biol Cell 16, 4531–4542.
Solis GP, Hoegg M, Munderloh C, Schrock Y, Malaga-Trillo E, Rivera-Milla E, Stuermer CA (2007). Reggie/flotillin proteins are organized into stable tetramers in membrane microdomains. Biochem J 403, 313–322.
Solis GP, Malaga-Trillo E, Plattner H, Stuermer CA (2010). Cellular roles of the prion protein in association with reggie/flotillin microdomains. Front Biosci 15, 1075–1085.
Sorkin A, Goh LK (2008). Endocytosis and intracellular trafficking of ErbBs. Exp Cell Res 314, 3093–3106.
Sorkin A, von Zastrow M (2009). Endocytosis and signalling: intertwining molecular networks. Nat Rev Mol Cell Biol 10, 609–622.
Stuermer CA (2010). The reggie/flotillin connection to growth. Trends Cell Biol 20, 6–13.
Stuermer CA, Langhorst MF, Wiechers MF, Legler DF, Von Hanwehr SH, Guse AH, Plattner H (2004). PrPc capping in T cells promotes its association with the lipid raft proteins reggie-1 and reggie-2 and leads to signal transduction. FASEB J 18, 1731–1733.
Tojima T, Hines JH, Henley JR, Kamiguchi H (2011). Second messengers and membrane trafficking direct and organize growth cone steering. Nat Rev Neurosci 12, 191–203.
Tominaga J, Fukunaga Y, Abelardo E, Nagafuchi A (2008). Defining the function of beta-catenin tyrosine phosphorylation in cadherin-mediated cell-cell adhesion. Genes Cells 13, 67–77.
Troyanovsky RB, Sokolov EP, Troyanovsky SM (2006). Endocytosis of cadherin from intracellular junctions is the driving force for cadherin adhesive dimer disassembly. Mol Biol Cell 17, 3484–3493.
Valdez G, Philippidou P, Rosenbaum J, Akmentin W, Shao Y, Halegoua S (2007). Trk-signaling endosomes are generated by Rac-dependent macroendocytosis. Proc Natl Acad Sci USA 104, 12270–12275.
Van Itallie CM, Balda MS, Anderson JM (1995). Epidermal growth factor induces tyrosine phosphorylation and reorganization of the tight junction protein ZO-1 in A431 cells. J Cell Sci 108, (Pt 4), 1735–1742.
Ware MF, Tice DA, Parsons SJ, Lauffenburger DA (1997). Overexpression of cellular Src in fibroblasts enhances endocytic internalization of epidermal growth factor receptor. J Biol Chem 272, 30185–30190.